Different effects of electronic excitation on metals and semiconductors

Gai-Qin Yan,[1] Xin-Lu Cheng,[1,2,*] Hong Zhang,[1,2,3] Zhi-Yang Zhu,[1] and Da-Hua Ren[1]
[1]*Institute of Atomic and Molecular Physics, Sichuan University, Chengdu 610065, China*
[2]*Key Laboratory of High Energy Density Physics and Technology of Ministry of Education, Sichuan University, Chengdu 610065, China*
[3]*College of Physical Science and Technology, Sichuan University, Chengdu 610065, China*
(Received 18 November 2015; revised manuscript received 12 May 2016; published 6 June 2016)

We study the electronic excitation effect upon ultrafast and intense laser irradiation on the stability of target materials, using density functional perturbation theory. The target materials include metals (Li, Na, Mg, Al, K, W, Au), Bi as a semimetal, and Si as a semiconductor. We found that the electronic excitation had different effects on the two distinct materials. For metals, the electronic pressure induces an increase in the shear modulus and presents a negative effect on the phonon entropy, which increases the lattice vibration frequency and melting temperature, leading to a higher stability for the close-packed structure (Al, Au, Mg). Conversely, the electronic pressure induces a decreasing trend in all these quantities, leading to a lower degree of stability and even a structural destabilization in the case of bcc-structured metals (W, Na, K, and Li). For semimetals and semiconductors, the internal pressure induces a completely opposite behavior with respect to close-packed structure metals. This can lead to structural destabilization for semimetals and even collapse for semiconductors. Finally, a shift of the Raman and infrared active modes is revealed for semimetals and semiconductors.

DOI: 10.1103/PhysRevB.93.214302

I. INTRODUCTION

Energy is first transferred to the electronic system when a solid surface is irradiated by intense femtosecond laser pulses, and then electrons thermalize to a temperature of about 10^4 K, leaving a "cold" lattice. The whole electron-lattice system is left in an out-of-equilibrium condition. Generally, intense femtosecond laser pulses can induce different physical effects on the materials, such as the excitation of coherent phonons [1,2], ultrafast solid-to-solid transitions [3–8], nonthermal melting [9–17], and phonon squeezing [18]. Typical structure responses can be classified into two distinct categories: nonthermal effects and thermal effects. Ultrafast nonthermal melting processes must occur in materials with an anomalous phase diagram with $dT_m/dP < 0$, where T_m is the melting temperature and P is pressure, such as in semiconductors and semimetals; while relatively slower thermal melting processes are the most favored mechanisms in all other materials, particularly, in materials having a normal phase diagram with $dT_m/dP > 0$, such as metals [19].

In semimetals and semiconductors, the potential energy surface notably changes under the effect of electronic excitation, inducing bond softening [20–25] and promoting the antibonding state character of the conduction band. A tight-binding model has been applied to study theoretically the instability of the diamond structure of Si, Ge, C, and GaAs due to a dense electron-hole plasma by Stampfli *et al.* [20,21]. By analyzing the phonon dispersion curve at different electronic temperatures, Recoules *et al.* [22] found an increase in lattice stability for metals, as opposed to its weakening in the case of semiconductors. Using the density functional linear-response theory, Feng *et al.* [26] studied the lattice instability of diamond structure semiconductors under intense laser irradiation. *Ab initio* molecular dynamics simulations under conditions of strong electronic excitation were performed on Si [25,27–30] and InSb [12,31,32], showing a destabilization of particular phonon branches of the lattice and the essentially athermal nature of the melting transition. By performing ultrafast x-ray diffraction probe experiments on laser-irradiated Ge, Siders *et al.* [33] directly observed the nonthermal loss of crystalline order both at the surface and in the bulk of the semiconductor lattice. Moreover, both theory and experiment showed a carrier-density-dependent lattice stability in semiconductors and semimetals. An increase in the photoexcited carrier density leads to a weakening in the crystal lattice, resulting in phonon softening with a decreased phonon frequency [34–37].

In the case of metals, the dominating process is thermal melting, and the force of interatomic interactions changes dramatically after laser irradiation. The hardening of bonds has been reported for Cu, Ag, and Au, while there is little change for Al and TiO_2 until the electronic temperature T_e reaches 6 eV. In the case of Mg, however, both softening and hardening of the bonds have been reported as a function of the electronic temperature [22,24,25,38,39]. Experiments of femtosecond electronic diffraction have captured the evidence for bond hardening in Au [40,41], and the ultrafast structure dynamics in warm dense matter has also provided a theoretical demonstration of interatomic bond strengthening in Cu and Ag, as a function of electronic temperature [38]. The temperature-dependent electronic thermophysical and thermodynamic properties of the eight representative metals (Al, Cu, Ag, Au, Ni, Pt, W, and Ti) are found to be very sensitive to details of the electronic structure of the material [42–44].

In this framework, it is mostly believed that phonons harden in metals and soften in semiconductors and semimetals. Moreover, little attention is currently being paid to the different origins of the stability of the whole system, especially for semimetals. In this paper, we will employ density functional perturbation theory (DFPT) to compute the evolution of the phonon spectrum of semiconductors, semimetals, and

*Corresponding author: chengxl@scu.edu.cn

representative metals (with fcc, bcc, and hcp structures) at different electronic temperatures. Afterwards, we will calculate the dynamical and thermodynamic properties of all these materials. We will demonstrate that both bond hardening and softening can occur in metals, where even instability can also emerge. In particular, the semimetal Bi exhibits a destabilization in particular phonon branches with an increase of the electronic temperature. Based on this fact, we will provide a deeper investigation of the physical origin of electronic excitation effects on different crystal structural stabilities.

II. COMPUTATIONAL DETAILS

A. Calculation scheme

All the calculations on the materials were performed with the Vienna *ab initio* simulation package (VASP) code [45–47] using the linear-response method, which is based on density functional theory (DFT), and the projector augmented wave method (PAW). In this paper, we use the PAW pseudopotential and the generalized gradient approximation (GGA) as the exchange-correlation functions designed by Perdew, Burke, and Ernzerhof (PBE) [42,48–50], which can deal with the exchange-correlation energy more effectively. The $3s^2 3p^1$, $5d^{10}6s^1$, $3s^2 3p^0$, $5d^4 6s^2$, $3s^1 3p^0$, $2s^1 2p^0$, $3s^2 3p^6 4s$ [1], $6s^2 6p^3$, and $3s^2 3p^2$ valence electrons have been treated explicitly for, respectively, Al, Au, Mg, W, Na, Li, K, Bi, and Si in the calculations, while the more tightly bound electrons are represented as core electrons. A plane-wave basis set with an energy cutoff of 500 eV was chosen to ensure a stable state of the system energy (except at 350 and 400 eV for Na and Bi, respectively). The Brillouin zone (BZ) was sampled by using $8 \times 8 \times 8$, $7 \times 7 \times 7$, $16 \times 16 \times 16$, $5 \times 5 \times 5$, and $6 \times 6 \times 6$ k meshes for metals (Li, Na, Al, K, Au), Mg, W, Bi, and Si according to the Monkhorst-Pack scheme [51]. Moreover, suitable bands were employed to ensure the availability of enough states for electrons to occupy even at high electronic temperatures. Phonon calculations were performed on a $2 \times 2 \times 2$ supercell. We have reoptimized the structure at T_e and our calculations are made at $V_{\mathrm{eq}}(T_e)$, as detailed in the Supplemental Material [52]. In addition, the thermodynamic functions were further evaluated at different electronic temperatures from the phonon dispersion relations and the phonon densities of states.

B. Finite-temperature density functional perturbation theory

There are two primary methods to calculate the phonon dispersion: the direct method and the linear-response method [53,54]. The direct method can be performed in two forms: the frozen-phonon method [55] and the force constant method [56,57]. The former is characterized by a drawback derived from the need to perform calculations in supercells, whose size depends on the commensurability of the perturbation with the unperturbed periodic cell. Another approach to the direct method uses the forces calculated via the Hellmann-Feynman theorem in the total energy calculations, deriving from them the values of the force constant matrices assuming a finite interaction range, and hence the dynamical matrix and phonon dispersion curves. The linear-response method, on the other hand, is based on the DFPT, which allows one to calculate the response of the electronic system to an applied perturbation self-consistently from first principles and to calculate the effect of strain on a system. According to the Hellmann-Feynman theorem, the second derivatives of the total energy with respect to atomic displacements can be obtained by the linear variation of the electron density upon application of an external static perturbation. The dynamical matrix, force constants, and phonon frequencies can subsequently be calculated from the obtained values for the forces and the displacements. Moreover, the DFPT approach to the calculation of phonon frequencies has the following peculiarity: The workload of the calculation is independent of phonon wavelength, since there is no connection between different wavelengths and the responses to perturbations.

Based on the application of the Hohenberg and Kohn theorem on many-body systems to the grand canonical ensemble designed by Mermin [58], the effects of electronic excitation were described by the dependent DFT which considers the electrons as thermalized and a Fermi-Dirac distribution as a function of the electronic temperature applied to the Kohn-Sham eigenstates. In this case, the electronic free-energy can be expressed as

$$F_{\mathrm{el}} = E - T_e S_{\mathrm{el}}, \tag{1}$$

and the electronic pressure can be expressed as

$$P_e = -\frac{\partial F}{\partial V} = -\frac{\partial E}{\partial V} + T_e \frac{\partial S_{\mathrm{el}}}{\partial V}, \tag{2}$$

$$S_{\mathrm{el}} = -k_B \int [f \ln f + (1-f)\ln(1-f)] n(E) dE, \tag{3}$$

where S_{el} is the electronic entropy, associated with the occupation of a state, f is the Fermi-Dirac distribution function, and $n(E)$ is the continuous presentation of the density of states.

C. Elastic properties

The elastic constants of a crystal are defined as the second derivatives of the total energy density with respect to the elements of the infinitesimal strain tensor. In this section, we calculated the total elastic moduli matrix directly with the stress-strain method based on DFT. The elastic stability of the structure is characterized by the Voigt average shear modulus. For cubic crystals, the Voigt average shear modulus $G = (3C_{44} + 2C')/5$, where C_{44} and $C' = (C_{11} - C_{12})/2$ are the two shear moduli of the cubic crystal. For hexagonal crystals $G = (M + 12C_{44} + 12C_{66})/30$, where $M = C_{11} + C_{12} + 2C_{33} - 4C_{13}$ and $C' = (C_{11} - C_{12})/2$. Using the elastic moduli, we can determine the Debye temperature Θ_D at different electronic temperatures, by using the following relation in a given volume V_m:

$$\Theta_D = \frac{\hbar}{k_B}\left[\frac{3n}{4\pi}\left(\frac{N_A \rho}{M}\right)\right]^{1/3} V_m. \tag{4}$$

The Debye-Lindemann theory assumes [22] that the melting temperature T_m is linked to Θ_D by the relation $T_m = A\Theta_D^2$, where A depends on the density and the atomic mass. The

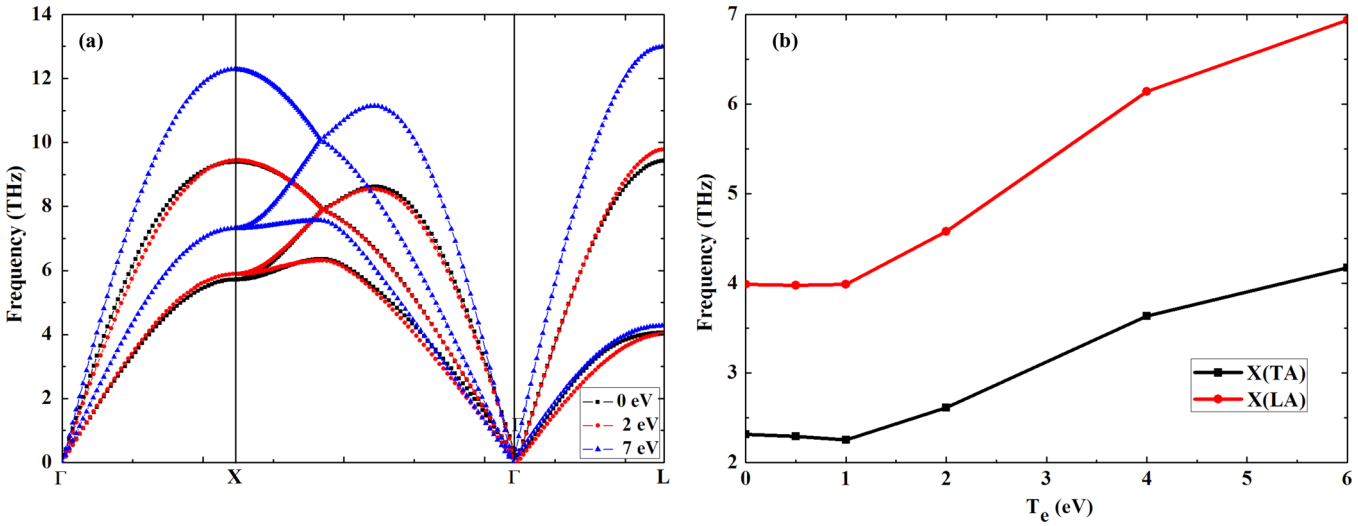

FIG. 1. (a) The phonon spectra of Al obtained at different electronic temperatures. (b) Phonon frequencies of the TA and LA modes for Au at high-symmetry X point as a function of the electronic temperature.

melting crystal temperature can be related to the electronic temperature by the following equation,

$$\frac{T_m}{T_{m_0}} = \left(\frac{\Theta_D}{\Theta_{D_0}}\right)^2. \tag{5}$$

III. RESULTS AND DISCUSSION

In order to study the effects of electronic excitation on the stability of the crystal structure, we calculated the dynamical and thermodynamic properties of semiconductors and metals. The phonon dispersion curves, the elastic moduli, and the melting temperature of the representative metals Li, Na, Mg, Al, K, W, Au, semimetal Bi, and semiconductor Si are plotted at different electronic temperatures.

A. fcc (Au, Al) and hcp crystals (Mg)

The phonon spectra of Al, which is a typical fcc-structured metal, are reported in Fig. 1(a) for different electronic temperatures. The phonon spectrum of Al shows a much smaller change upon excitation, while the phonon frequency of Au, shown in Fig. 1(b), has a prominent increase with an increase in electronic temperature. Furthermore, it is possible to notice that the phonon frequency of Al decreases by a little amount below $T_e = 2$ eV, and then increases until $T_e = 7$ eV. However, the phonon frequency of Au decreases slightly below $T_e = 1$ eV; these results are nearly consistent with those demonstrated by Darascewicz *et al.* [59]. Moreover, the rate of change in the phonon frequency of Au gradually decreases when the electronic temperature is above 4 eV. These results are nearly consistent with the results from Recoules *et al.* [22].

Figure 2 shows the elastic constant C', bulk modulus B_0, shear modulus G_0, Young's modulus E_0, Debye temperature Θ_D, and melting temperature T_m of Al and Au as a function of the electronic temperature. In the case of Au, an increase in the electronic temperature leads to higher values for both the melting temperature T_m and the Debye temperature Θ_D, as well as an increase in the elastic moduli. The trend for Al,

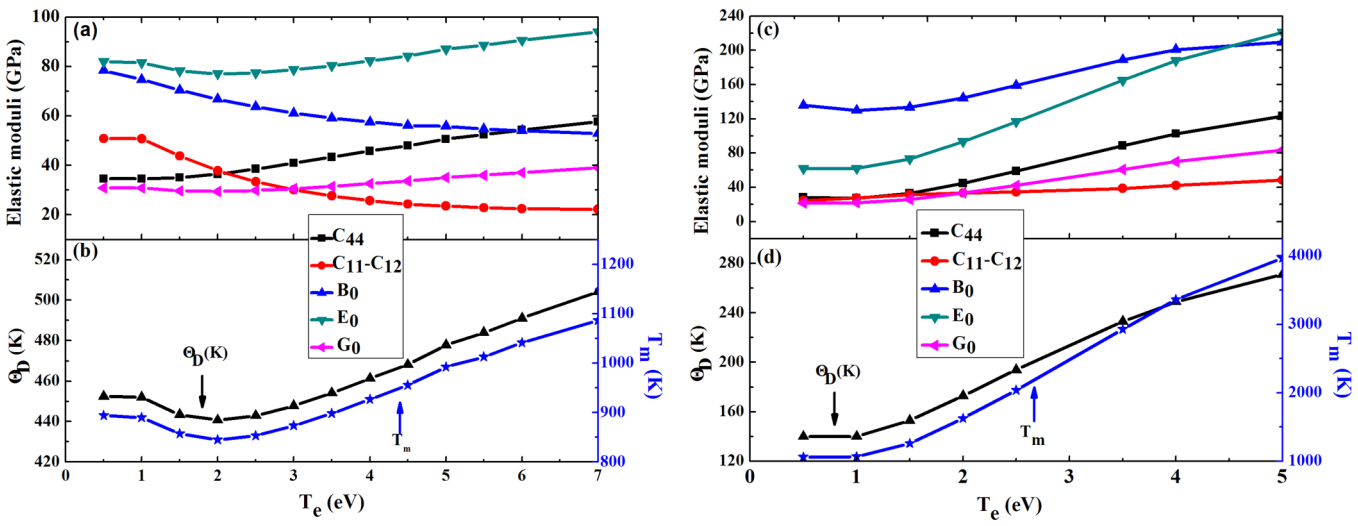

FIG. 2. Electronic temperature-dependent elastic moduli, Debye temperature Θ_D, and melting temperature T_m in (a) Al and (b) Au.

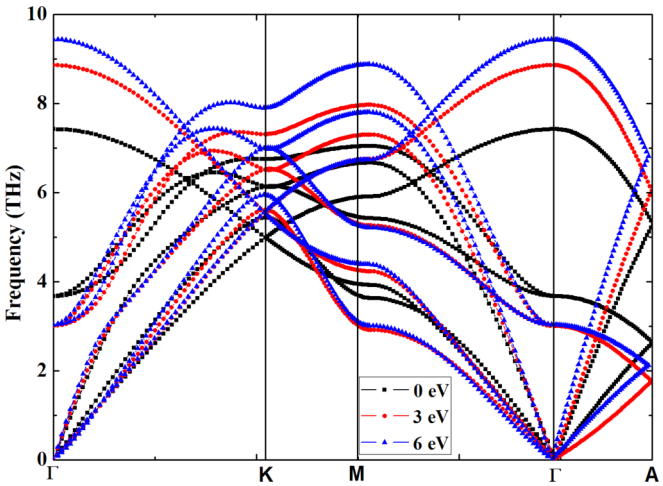

FIG. 3. The phonon spectra of Mg obtained at different electronic temperatures.

however, is different: The elastic constant C' and bulk modulus B_0 gradually decrease until $T_e = 7$ eV, while the melting temperature T_m, shear modulus G_0, and Young's modulus E_0 decrease below $T_e = 2$ eV, and then increase at higher electronic temperatures. Moreover, the melting temperature T_m and Debye temperature Θ_D decrease below $T_e = 2$ eV, and then begin to increase with increasing T_e. By noting the similarities in phonon frequency variations, we can conclude that fcc-structured metals eventually become more stable under electronic excitation.

We also studied the dynamics of Mg as a hexagonal-structured metal, as shown in Fig. 3. The transverse acoustic (TA) phonon frequencies decrease below $T_e = 3$ eV at the M and A points, and then increase for electronic temperatures up to 6 eV. Conversely, the longitudinal optical (LO) phonon frequencies increase monotonically with the electronic temperature. The elastic constant, elastic modulus, Debye temperature Θ_D, and melting temperature T_m of Mg show a similar trend with the variations of the phonon spectrum. Therefore, the crystal structure becomes more stable under strong electronic excitation.

For a deeper investigation of the physical origin of electronic excitation effects, we present the relationship between the electronic free energy F, the electronic internal energy E, and the volume V at different electronic temperatures for Al. Figures 4(a) and 4(b) show that the gradient presents a positive trend in the temperature range from $T_e = 300$ to 10 000 K, and it suggests that the electronic internal energy provides the primary contribution to the free energy, which can be attributed to an enhancement of the thermal excitation of electrons on the electron specific heat of metals [43]. However, the F-V curve has a negative gradient and continues to increase with V, and the E-V curve maintains the same gradient when T_e is above 20 000 K. According to Eqs. (2) and (3), the electron entropy S_e undergoes a significant modification as a consequence of changes in the density of states, and the increase of S_e affects the electron external pressure P_e, which contributes to the thermal melting of the crystal. Namely, P_e directly yields effects on the stress state of a solid in the presence of lattice strain, leading to an increase in the shear modulus and in the hardening of the transverse acoustic phonon frequency as the electronic temperature increases, and eventually to an improvement of the stability of the system.

From Figs. 4(c) and 4(d), we can see that both phonon entropy S and phonon heat capacity C_v increase with the lattice temperature. Moreover, the electronic excitation negatively affects both quantities. The smaller uncertainty associated with a random variable leads to an increase in the melting temperature. In other words, investigations on the phonon entropy S confirm the stability of the lattice under strong electronic excitation.

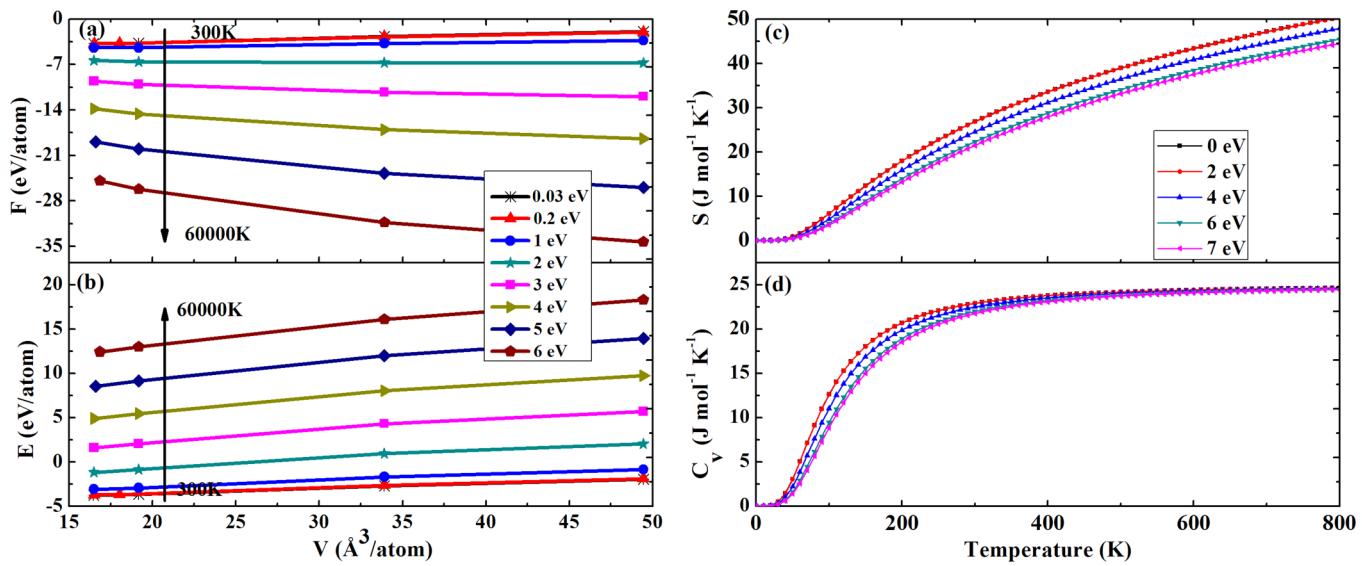

FIG. 4. (a) Electronic free energy F and (b) electronic internal energy E as a function of the volume V of Al at different electronic temperatures; the arrow points in the direction of the electronic temperature increasing from 300 to 60 000 K. The lines correspond to $T_e = 300$, 2000, 10 000, 20 000, 30 000, 40 000, 50 000, and 60 000 K, respectively. (c) The phonon entropy S and (d) phonon heat capacity C_v of Al at different electronic temperatures.

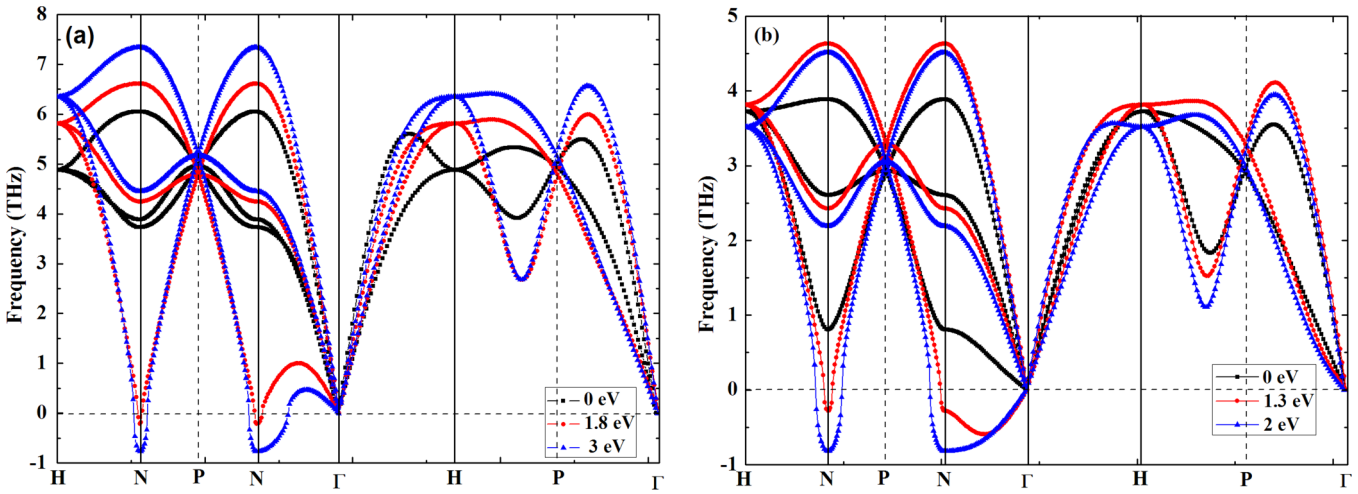

FIG. 5. The phonon spectra of (a) W and (b) Na obtained as a function of the electronic temperature T_e.

B. bcc crystals (W, Na, K, Li)

The variation of the lattice vibration frequency provides important information about the lattice dynamic stability. As shown in Fig. 5(a), variations of the lattice vibration frequency of bcc-structured W are characterized by the opposite trend as a function of electronic temperature with respect to what was found for the fcc structures, reported in Fig. 1(a). The phonon frequencies decrease along the Γ-N line as the electronic temperature is increased. In particular, when the target materials reach $T_e = 1.8$ eV, the mode of the transverse acoustic branch along the Γ-N line begins to exhibit an imaginary frequency contribution, which is maintained up to $T_e = 3$ eV, suggesting a destabilization of the lattice. Conversely, the change of longitudinal acoustic (LA) branch phonon frequencies can be neglected. This can allow that the crystals occur at a slight instability.

In addition, we also calculated the elastic constant, elastic modulus, and melting temperature T_m of W as a function of the electronic temperature; results are presented in Figs. 6(a) and 6(b). All the computed quantities exhibit a slightly decreasing trend in the case of W, except for the elastic constant C_{44}. Still, we note that the stability of the crystal structure decreases as a consequence of the decrease in the shear modulus G_0. As found in previous works [60], the elastic constant C' decrease is a typical pretransition phenomenon related to the transition from a bcc to a close-packed structure. Here, C' is close to zero, which may indicate the onset of a phase transition for W. Moreover, both the Debye temperature Θ_D and the melting temperature T_m decrease, which is attributed to the destabilized lattice resulting from the decrease in the elastic modulus and the softening of the phonon modes of the material.

The primary mechanism was investigated with the same approach as was adopted for Al and Au. Namely, the electron external pressure P_e directly affects the lattice stress state, leading to a decrease of the elastic modulus with increasing electronic temperature. The lattice becomes destabilized and the system eventually achieves a slight instability.

Similar dynamics calculations were carried out for the bcc crystal structure Na, finding a similar trend. It is thus possible to hypothesize that the electronic excitation may promote stability in fcc structures while restraining the stability for

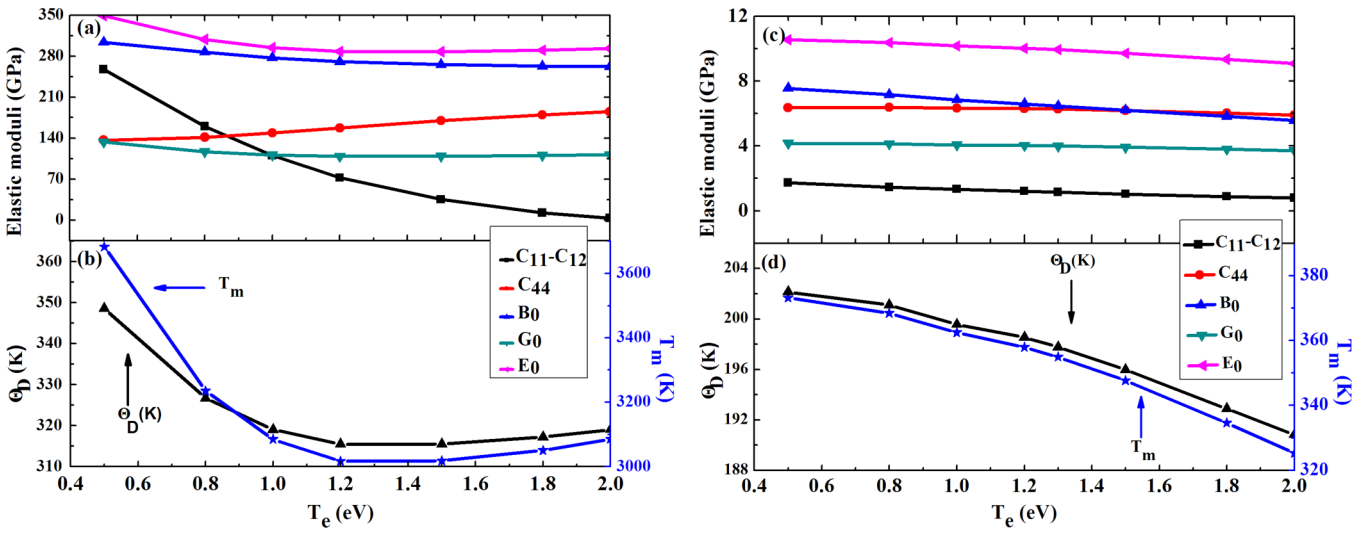

FIG. 6. Electronic temperature-dependent elastic moduli, Debye temperature Θ_D, and melting temperature T_m in (a) W and (b) Na.

bcc structures. The same approach was adopted to calculate the dynamics for the same group elements Li and K, which are found as both bcc and fcc crystal structures at normal temperatures. The transverse acoustic phonon frequency exhibits a slight decrease or increase. C' decreases for the bcc phase and increases for the fcc phase, providing confirmation of the fact that bcc structures have a lower stability compared with close-packed structures. Moreover, imaginary phonon frequencies appear at $T_e = 0$ eV for Li, disappearing when $T_e = 0.75$ eV; we can attribute this to the electron pressure which leads the unsteady bcc phase towards stability.

To summarize, electronic excitation enhances the stability of the close-packed crystal structure, showing a moderate effect on the materials having bcc and fcc crystal structures, whereas bcc crystal structures exhibit a lower degree of stability, even becoming unstable below $T_e = 3$ eV. This can be explained by noting that the bcc structure is more open than the close-packed structure. As a result, a bcc structure is more likely to undergo a structure transition towards an fcc structure under electronic excitation. Eventually, it is possible to hypothesize that the crystal structure could undergo nonthermal solid-to-solid phase transitions from bcc to form a close-packed structure above $T_e = 3$ eV.

C. Semimetal (Bi) and semiconductor (Si)

In the case of rhombohedral structure Bi, the optical and acoustic phonon frequencies both decrease in the range from $T_e = 0$ to 1.2 eV, as shown in Fig. 7(a).The acoustic modes are not strongly affected by electronic excitation, except at the A point, while there is a visible decrease in optical mode frequencies. These results are consistent with the dispersion curves from rhombohedral $A7$ phase Bi presented by Murray *et al.* [36]. Furthermore, the A_{1g} mode of the LO branch exhibits a redshift from the equilibrium value under electronic excitation, indicating the effect of phonon softening, and the E_g mode of LA branch shows a blueshift towards the equilibrium value. This is consistent with the results measured from rhombohedral $A7$ phase Bi [34]. Above $T_e = 1.2$ eV, the mode of the transverse acoustic branch along the Γ-K-M line begins to include an imaginary frequency, which suggests destabilization of the lattice. The band gap of the phonon mode is 0.879 THz at room temperature, and its value increases with electronic temperature until $T_e = 2.7$ eV, except for electronic temperatures approaching 1.2 eV, which almost leads to the disappearance of the phonon band gap.

In addition, Gonze *et al.* [61] demonstrated that spin-orbit coupling (SOC) has a softening effect on all the phonon frequencies. We calculated the SOC effect on the phonon spectra at different electronic temperatures. Compared to the phonon spectrum without SOC at $T_e = 1.2$ eV as shown in Fig. 7(b), we found that SOC induced a slight decrease in the optical mode frequencies. The effect on the transverse acoustic branch mode can be ignored. Moreover, the transverse acoustic branch mode with SOC along the Γ-K-M line also shows the beginning of an imaginary frequency at $T_e = 1.2$ eV. In other words, the effect of SOC on the stability of Bi can be ignored.

As can be seen in Fig. 7(a), the phonon frequency undergoes a redshift which leads to an asymmetric broadening on the phonon density of states towards the lower-frequency side. Therefore, the unique low-frequency tail of the phonon density of states at higher electronic temperatures suggests a substantial phonon mode softening.

The properties of bulk Bi are linked to its peculiar electronic structure with a tiny electron and a portion of hole. The relatively localized valence holes are redistributed between the nearest-neighbor atoms at high electronic temperatures. Local changes in hole density lead to changes in interatomic interactions, resulting in a large internal pressure P [19], which affects the stress state of a solid in the presence of lattice strain. The strong force acting on the atoms can accelerate their motion along the longitudinal direction of the lattice, enhancing the degree of coupling between the A_{1g} and the E_g modes, or longitudinal and unstable transverse vibrational modes. This can result in a stability decrease. On the other hand, as a consequence of the thermal excitation

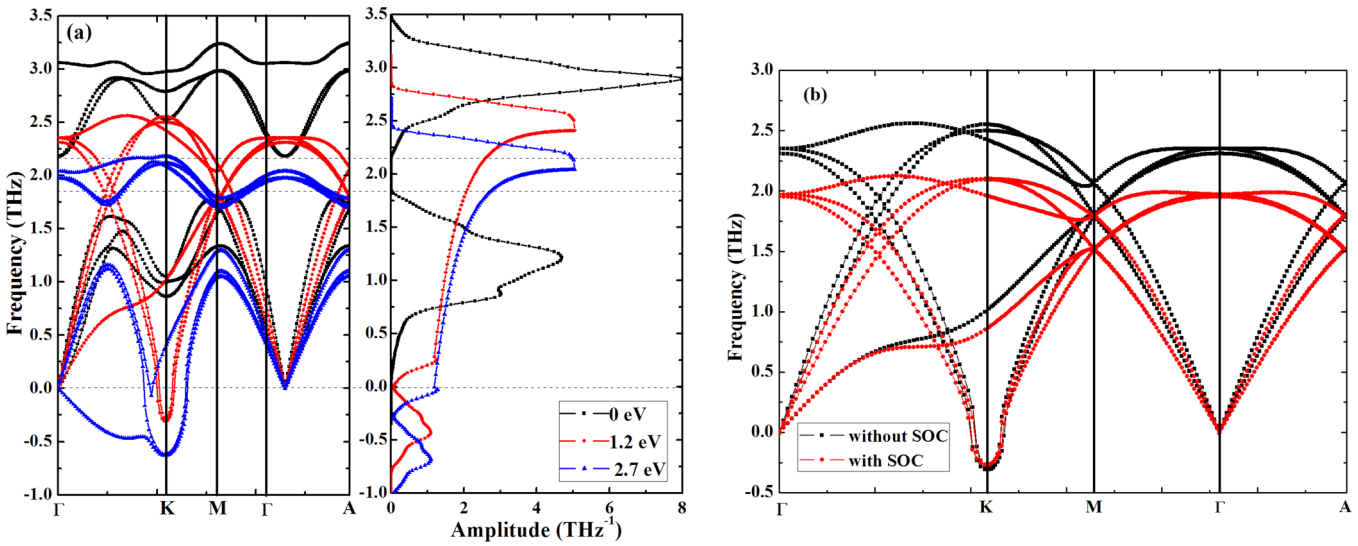

FIG. 7. (a) The phonon spectra and phonon densities of states with respect to the rhombohedral Bi obtained at different electronic temperatures. (b) The phonon spectra with respect to the rhombohedral Bi obtained at $T_e = 1.2$ eV.

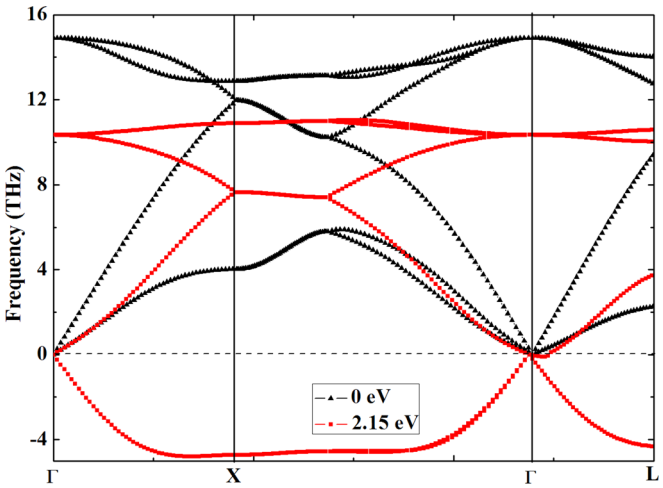

FIG. 8. The phonon spectra of Si obtained at different electronic temperatures.

of the electrons, the external pressure P_e induces electrons to move out of their bonding states. Therefore, both internal and external pressures concur in destabilizing the lattice. Moreover, the localized stress leads to a redshift of all the Raman active modes, whereas the infrared active modes undergo a redshift below $T_e = 1.5$ eV, followed by a blueshift at higher electronic temperatures.

Figure 8 shows the phonon spectra of Si at different electronic temperatures. The optical and acoustic phonon frequencies both decrease for electronic temperatures up to 1.5 eV. At higher temperatures, the transverse acoustic phonon frequencies along the Γ-X line begin to exhibit imaginary frequencies, indicating that the lattice is becoming unstable. Furthermore, when $T_e = 2.15$ eV, the whole transverse acoustic phonon mode in the full Brillouin zone becomes imaginary, which suggests that the lattice may be shrinking or even collapsing. Finally, it is possible to notice that the phonon frequency of the longitudinal optical branch decreases all along.

The elastic constant and elastic modulus of Si show significant variations as a function of the electronic temperature, steadily decreasing when it reaches the characteristic value $T_e = 1.5$ eV, while the frequency of the transverse acoustic mode becomes imaginary and C' becomes negative, as shown in Fig. 9. The transverse acoustic mode gradually evolves towards a completely imaginary frequency. However, the value of C' is small enough to result in the local destabilization of the lattice, with the subsequent onset of a phase transition. Similar trends were observed for the average shear modulus G_0, which can support the interpretation according to which lattice instability is favored by a decrease in the shear moduli. The strength of the bond corresponding to a characteristic Raman peak becomes weaker, due to the localized stress which leads to a redshift of the Raman active modes. We also found that electronic excitation shows a positive effect on the phonon entropy S and phonon heat capacity C_v, which leads to a decrease in the melting temperature. In other words, the phonon entropy S and phonon heat capacity C_v support our results on the instability of the lattice under strong electronic excitation.

Similarly to the semimetal Bi, local changes in the hole density determine a large internal pressure P for the semiconductor Si [19]. This pressure can cause the lattice to shrink and eventually collapse with decreasing the shear moduli. The phonon frequency of the longitudinal optical branch decreases, and enhances the effective instability of the Si crystal by means of coupling to the unstable acoustic branch phonon mode.

IV. SUMMARY

The different effects of electronic excitation on metals and semiconductors are presented. For metals, due to the thermal excitation of the electrons, the electron entropy S_e undergoes significant modifications with changes in the density of states. The increase of S_e generates an electron external pressure P_e, which leads to an increase in phonon vibration frequencies and elastic modulus with a close-packed structure. Meanwhile, the melting temperature of crystals increases with the electronic temperature, which has a positive effect on the stability of

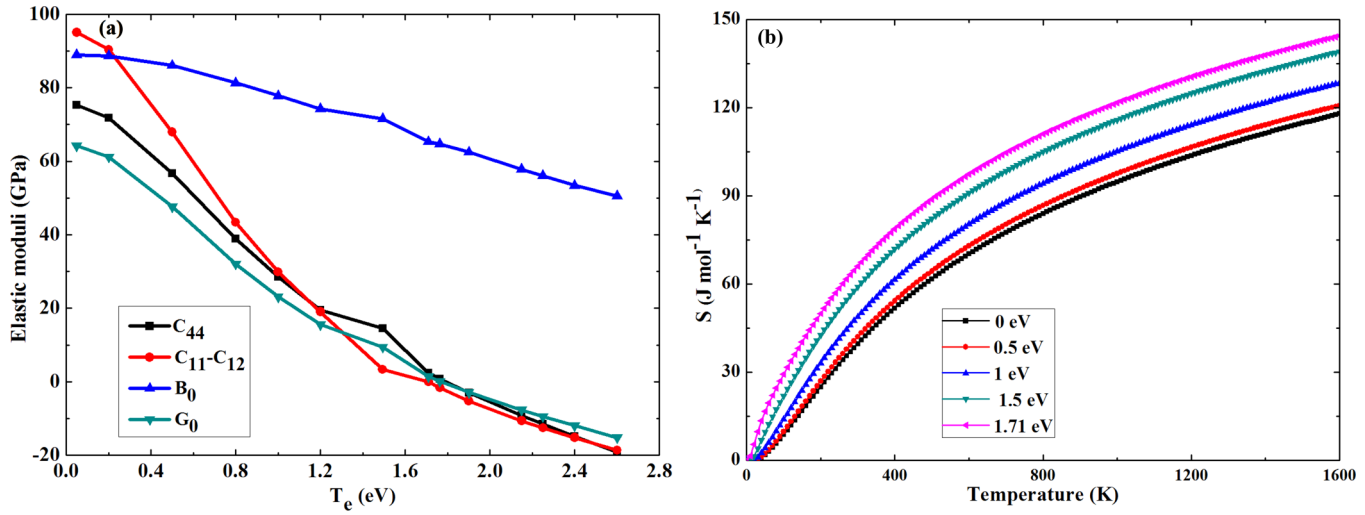

FIG. 9. (a) Electronic temperature-dependent elastic moduli of Si. (b) The phonon entropy S of Si at different electronic temperatures.

the crystal structure. On the other hand, the electron external pressure P_e induces an opposite trend in all these quantities compared with the close-packed structure, with a lower degree of stability, even leading to a structural destabilization at higher electronic temperatures for the bcc crystal structure. Moreover, the electron external pressure P_e also leads to the stability of the crystal structure to decrease or increase slightly for the materials having a bcc or fcc crystal structure. This behavior can be attributed to the fact that the bcc structure is more open than the close-packed structure and it is thus more likely to experience a structure transition. Furthermore, the thermodynamic properties including phonon entropy S and phonon heat capacity C_v support our evidence on the stability of the lattice under electronic excitation.

However, for semiconductors and semimetals, due to the thermal excitation of the electrons, local changes in the hole density lead to changes in the interatomic interactions. This gives rise to a large internal pressure P. This pressure can decrease the elastic constant and soften the phonon mode, leading to the instability of the crystal lattice for semimetal Bi, and eventually to its collapse for semiconductor Si. Meanwhile, the optical branch accelerates the instability by means of coupling to the unstable acoustic branch phonon mode. In addition, the localized stress leads to a shift of the Raman active and infrared active modes for the semiconductor and the semimetal we have considered. Electronic excitation presents a positive effect on the phonon entropy S and phonon heat capacity C_v, further verifying the instability of the lattice under strong electronic excitation.

ACKNOWLEDGMENT

We acknowledge financial support from the National Natural Science Foundation of China (Grants No. 11374217 and No. 11474207).

[1] H. J. Zeiger, J. Vidal, T. K. Cheng, E. P. Ippen, G. Dresselhaus, and M. S. Dresselhaus, Phys. Rev. B **45**, 768 (1992).
[2] R. Merlin, Solid State Commun. **102**, 207 (1997).
[3] H. O. Jeschke, M. E. Garcia, and K. H. Bennemann, Phys. Rev. B **60**, R3701(R) (1999).
[4] H. O. Jeschke, M. E. Garcia, and K. H. Bennemann, J. Appl. Phys. **91**, 18 (2002).
[5] A. Cavalleri, Cs. Toth, C. W. Siders, J. A. Squier, F. Raksi, P. Forget, and J. C. Kieffer, Phys. Rev. Lett. **87**, 237401 (2001).
[6] R. Kitagawa, H. Takebe, and K. Morinaga, Appl. Phys. Lett. **82**, 3641 (2003).
[7] E. S. Zijlstra, N. Huntemann, and M. E. Garcia, New J. Phys. **10**, 033010 (2008).
[8] M. S. Diakhate and M. E. Garcia, Phys. Rev. B **79**, 094117 (2009).
[9] S. L. Johnson, P. A. Heimann, A. M. Lindenberg, H. O. Jeschke, M. E. Garcia, Z. Chang, R. W. Lee, J. J. Rehr, and R. W. Falcone, Phys. Rev. Lett. **91**, 157403 (2003).
[10] H. O. Jeschke, M. E. Garcia, M. Lenzner, J. Bonse, J. Krüger, and W. Kautek, Appl. Surf. Sci. **197**, 839 (2002).
[11] A. Rousse, C. Rischel, S. Fourmaux, I. Uschmann, S. Sebban, G. Grillon, P. Balcou, E. Förster, J. P. Geindre, P. Audebert, J. C. Gauthier, and D. Hulin, Nature (London) **410**, 65 (2001).
[12] A. M. Lindenberg, J. Larsson, K. Sokolowski-Tinten, K. J. Gaffney, C. Blome, O. Synnergren, J. Sheppard, C. Caleman, A. G. MacPhee, D. Weinstein, D. P. Lowney, T. K. Allison, T. Matthews, A. L. Cavalieri, D. M. Fritz, S. H. Lee, P. H. Bucksbaum, D. A. Reis, J. Rudati, P. H. Fuoss, C. C. Kao, D. P. Siddons, R. Pahl, J. Als-Nielsen, S. Duesterer, R. Ischebeck, H. Schlarb, H. Schulte-Schrepping, T. Tschentscher, J. Schneider, D. von der Linde, O. Hignette, F. Sette, H. N. Chapman, R. W. Lee, T. N. Hansen, S. Techert, J. S. Wark, M. Bergh, G. Huldt, D. van der Spoel, N. Timneanu, J. Hajdu, R. A. Akre, E. Bong, P. Krejcik, J. Arthur, S. Brennan, K. Luening, and J. B. Hastings, Science **308**, 392 (2005).
[13] E. S. Zijlstra, J. Walkenhorst, and M. E. Garcia, Phys. Rev. Lett. **101**, 135701 (2008).
[14] S. Q. Feng, J. L. Zhao, X. L. Cheng, and H. Zhang, J. Appl. Phys. **114**, 043519 (2013).
[15] M. Harb, R. Ernstorfer, C. T. Hebeisen, G. Sciaini, W. Peng, T. Dartigalongue, M. A. Eriksson, M. G. Lagally, S. G. Kruglik, and R. J. D. Miller, Phys. Rev. Lett. **100**, 155504 (2008).
[16] T. Dumitrică and R. E. Allen, Phys. Rev. B **66**, 081202(R) (2002).
[17] J. P. Callan, A. M. T. Kim, L. Huang, and E. Mazur, Chem. Phys. **251**, 167 (2002).
[18] X. D. Hu and F. Nori, Phys. Rev. Lett. **79**, 4605 (1997).
[19] H. Hu, H. P. Ding, and F. Liu, Sci. Rep. **5**, 8212 (2015).
[20] P. Stampfli and K. H. Bennemann, Phys. Rev. B **42**, 7163 (1990).
[21] P. Stampfli and K. H. Bennemann, Phys. Rev. B **49**, 7299 (1994).
[22] V. Recoules, J. Clérouin, G. Zérah, P. M. Anglade, and S. Mazevet, Phys. Rev. Lett. **96**, 055503 (2006).
[23] E. S. Zijlstra, L. L. Tatarinova, and M. E. Garcia, Phys. Rev. B **74**, 220301(R) (2006).
[24] E. S. Zijlstra, F. C. Kabeer, B. Bauerhenne, T. Zier, N. Grigoryan, and M. E. Garcia, Appl. Phys. A **110**, 519 (2013).
[25] N. S. Grigoryan, T. Zier, M. E. Garcia, and E. S. Zijlstra, J. Opt. Soc. Am. B **31**, C22 (2014).
[26] S. Q. Feng, J. L. Zhao, and X. L. Cheng, J. Appl. Phys. **113**, 023301 (2013).
[27] L. Shokeen and P. K. Schelling, Appl. Phys. Lett. **97**, 151907 (2010).
[28] P. L. Silvestrelli, A. Alavi, M. Parrinello, and D. Frenkel, Phys. Rev. Lett. **77**, 3149 (1996).
[29] P. L. Silvestrelli, A. Alavi, M. Parrinello, and D. Frenkel, Phys. Rev. B **56**, 3806 (1997).
[30] A. Gambirasio, M. Bernasconi, and L. Colombo, Phys. Rev. B **61**, 8233 (2000).
[31] K. J. Gaffney, A. M. Lindenberg, J. Larsson, K. Sokolowski-Tinten, C. Blome, O. Synnergren, J. Sheppard, C. Caleman, A. G. MacPhee, D. Weinstein, D. P. Lowney, T. Allison, T. Matthews, R. W. Falcone, A. L. Cavalieri, D. M. Fritz, S. H. Lee, P. H. Bucksbaum, D. A. Reis, J. Rudati, A. T. Macrander,

P. H. Fuoss, C. C. Kao, D. P. Siddons, R. Pahl, K. Moffat, J. Als-Nielsen, S. Duesterer, R. Ischebeck, H. Schlarb, H. Schulte-Schrepping, J. Schneider, D. von der Linde, O. Hignette, F. Sette, H. N. Chapman, R. W. Lee, T. N. Hansen, J. S. Wark, M. Bergh, G. Huldt, D. van der Spoel, N. Timneanu, J. Hajdu, R. A. Akre, E. Bong, P. Krejcik, J. Arthur, S. Brennan, K. Luening, and J. B. Hastings, Phys. Rev. Lett. **95**, 125701 (2005).

[32] P. B. Hillyard, K. J. Gaffney, A. M. Lindenberg, S. Engemann, R. A. Akre, J. Arthur, C. Blome, P. H. Bucksbaum, A. L. Cavalieri, A. Deb, R. W. Falcone, D. M. Fritz, P. H. Fuoss, J. Hajdu, P. Krejcik, J. Larsson, S. H. Lee, D. A. Meyer, A. J. Nelson, R. Pahl, D. A. Reis, J. Rudati, D. P. Siddons, K. Sokolowski-Tinten, D. von der Linde, and J. B. Hastings, Phys. Rev. Lett. **98**, 125501 (2007).

[33] C. W. Siders, A. Cavalleri, K. Sokolowski-Tinten, Cs. Toth, T. Guo, M. Kammler, M. Horn von Hoegen, K. R. Wilson, D. von der Linde, and C. P. J. Barty, Science **286**, 1340 (1999).

[34] D. M. Fritz, D. A. Reis, B. Adams, R. A. Akre, J. Arthur, C. Blome, P. H. Bucksbaum, A. L. Cavalieri, S. Engemann, S. Fahy, R. W. Falcone, P. H. Fuoss, K. J. Gaffney, M. J. George, J. Hajdu, M. P. Hertlein, P. B. Hillyard, M. Horn-von Hoegen, M. Kammler, J. Kaspar, R. Kienberger, P. Krejcik, S. H. Lee, A. M. Lindenberg, B. McFarland, D. Meyer, T. Montagne, É. D. Murray, A. J. Nelson, M. Nicoul, R. Pahl, J. Rudati, H. Schlarb, D. P. Siddons, K. Sokolowski-Tinten, Th. Tschentscher, D. von der Linde, and J. B. Hastings, Science **315**, 633 (2007).

[35] E. S. Zijlstra, L. E. Diaz-Sanchez, and M. E. Garcia, Phys. Rev. Lett. **104**, 029601 (2010).

[36] É. D. Murray, S. Fahy, D. Prendergast, T. Ogitsu, D. M. Fritz, and D. A. Reis, Phys. Rev. B **75**, 184301 (2007).

[37] G. Sciaini, M. Harb, S. G. Kruglik, T. Payer, C. T. Hebeisen, F. J. M. zu Heringdorf, M. Yamaguchi, M. H. von Hoegen, R. Ernstorfer, and R. J. D. Miller, Nature (London) **458**, 07788 (2009).

[38] F. Cheenicode Kabeer, E. S. Zijlstra, and M. E. Garcia, Phys. Rev. B **89**, 100301(R) (2014).

[39] N. S. Grigoryan, E. S. Zijlstra, and M. E. Garcia, New J. Phys. **16**, 013002 (2014).

[40] R. Ernstorfer, M. Harb, C. T. Hebeisen, G. Sciaini, T. Dartigalongue, and R. J. D. Miller, Science **323**, 20 (2009).

[41] C. Fourment, F. Deneuville, D. Descamps, F. Dorchies, S. Petit, O. Peyrusse, B. Holst, and V. Recoules, Phys. Rev. B **89**, 161110(R) (2014).

[42] E. Bévillon, J. P. Colombier, V. Recoules, and R. Stoian, Phys. Rev. B **89**, 115117 (2014).

[43] Z. Lin, L. V. Zhigilei, and V. Celli, Phys. Rev. B **77**, 075133 (2008).

[44] B. Y. Mueller and B. Rethfeld, Phys. Rev. B **87**, 035139 (2013).

[45] W. Kohn and L. J. Sham, Phys. Rev. **140**, A1133 (1965).

[46] G. Kresse and D. Joubert, Phys. Rev. B **59**, 1758 (1999).

[47] G. Kresse and J. Furthmuller, Phys. Rev. B **54**, 11169 (1996).

[48] V. N. Staroverov, G. E. Scuseria, J. P. Perdew, E. R. Davidson, and J. Katriel, Phys. Rev. A **74**, 044501 (2006).

[49] Z. G. Wu and R. E. Cohen, Phys. Rev. B **73**, 235116 (2006).

[50] J. P. Perdew, K. Burke, and M. Ernzerhof, Phys. Rev. Lett. **77**, 3865 (1996).

[51] H. J. Monkhorst and J. D. Pack, Phys. Rev. B **13**, 5188 (1976).

[52] See Supplemental Material at http://link.aps.org/supplemental/10.1103/PhysRevB.93.214302 for details on lattice parameters at different electronic temperatures Te for W.

[53] P. Giannozzi, S. de Gironcoli, P. Pavone, and S. Baroni, Phys. Rev. B **43**, 7231 (1991).

[54] X. Gonze and C. Lee, Phys. Rev. B **55**, 10355 (1997).

[55] K. Kunc and R. M. Martin, Phys. Rev. Lett. **48**, 406 (1982).

[56] G. Kresse, J. Furthmüller, and J. Hafner, Europhys. Lett. **32**, 729 (1995).

[57] K. Parlinski, Z.-Q. Li, and Y. Kawazoe, Phys. Rev. Lett. **78**, 4063 (1997).

[58] N. D. Mermin, Phys. Rev. **137**, A1441 (1965).

[59] S. L. Daraszewicz, Y. Giret, N. Naruse, Y. Murooka, J. F. Yang, D. M. Duffy, A. L. Shluger, and K. Tanimura, Phys. Rev. B **88**, 184101 (2013).

[60] M. I. Katsnelson, I. I. Naumov, and A. V. Trefilov, Phase Transitions **49**, 143 (1994).

[61] L. E. Díaz-Sánchez, A. H. Romero, and X. Gonze, Phys. Rev. B **76**, 104302 (2007).